tvst

Article

Tissue Plasminogen Activator Effects on Fibrin Volume and the Ocular Proteome in a Juvenile Rabbit Model of Lensectomy

Jonathon B. Young[1], Amanda Rae Buchberger[2,3], Joseph D. Bogaard[4], Linda Berg Luecke[5–8], Matthew Runquist[9], Christine M. B. Skumatz[4], and Iris S. Kassem[1,4]

[1] Cell Biology, Neurobiology and Anatomy, Medical College of Wisconsin, Milwaukee, WI, USA
[2] Center for Biomedical Mass Spectrometry Research, Medical College of Wisconsin, Milwaukee, WI, USA
[3] Chemistry, University of Wisconsin–Madison, Madison, WI, USA
[4] Ophthalmology and Visual Sciences, Medical College of Wisconsin, Milwaukee, WI, USA
[5] Department of Biochemistry, Medical College of Wisconsin, Milwaukee, WI, USA
[6] CardiOmics Program, Center for Heart and Vascular Research, University of Nebraska Medical Center, Omaha, NE, USA
[7] Division of Cardiovascular Medicine, Department of Internal Medicine, University of Nebraska Medical Center, Omaha, NE, USA
[8] Department of Cellular and Integrative Physiology, University of Nebraska Medical Center, Omaha, NE, USA
[9] Department of Radiology, Medical College of Wisconsin, Milwaukee, WI, USA

Correspondence: Iris S. Kassem, Cell Biology, Neurobiology and Anatomy, Medical College of Wisconsin Eye Institute, 925 N. 87th Street, Milwaukee, WI 53226, USA.
e-mail: ikassem@mcw.edu

Received: December 21, 2020
Accepted: August 31, 2021
Published: December 7, 2021

Keywords: fibrin; aqueous humor; mass spectrometry; magnetic resonance imaging

Citation: Young JB, Buchberger AR, Bogaard JD, Luecke LB, Runquist M, Skumatz CMB, Kassem IS. Tissue plasminogen activator effects on fibrin volume and the ocular proteome in a juvenile rabbit model of lensectomy. Transl Vis Sci Technol. 2021;10(14):7, https://doi.org/10.1167/tvst.10.14.7

Purpose: To investigate the use of tissue plasminogen activator (tPA) and its effects on the ocular proteome as a therapeutic intervention for postoperative inflammation and fibrin formation following intraocular lens (IOL) insertion in a juvenile rabbit model.

Methods: Twenty-six rabbits, 6 to 7 weeks old, underwent lensectomy with IOL insertion. Following examination on day 3, 100 µL of either 25 µg of recombinant rabbit tPA or balanced salt solution (control) was injected into the anterior chamber. On postoperative day 4, rabbits underwent examination, and eyes were harvested and fixed for 9.4-Tesla magnetic resonance imaging (MRI). Three masked observers quantified fibrin scar volume using Horos Project software. Aqueous humor (AH) was collected immediately prior to surgery and on postoperative days 3 and 4. Proteins related to coagulation and inflammation were assessed in AH samples using targeted mass spectrometry via parallel reaction monitoring.

Results: tPA significantly reduced the volume of fibrin 24 hours following administration compared with control eyes (0.560 mm^3 vs. 3.29 mm^3; $P < 0.0001$). Despite the reduced fibrin scar, proteins related to the coagulation and complement cascade were not significantly different following tPA injection.

Conclusions: tPA may be a safe candidate for reduction of postoperative fibrin scarring after intraocular surgery. MRI can provide a quantitative value for fibrin volume changes.

Translational Relevance: tPA is a candidate to treat ocular fibrin scarring. MRI can quantify the efficacy of treatments in future dose-response studies. Targeted mass spectrometry can provide critical data necessary to help decipher the effect on the abundance of targeted proteins following pharmacological intervention.

Introduction

Cataracts remain a prevalent cause of blindness across the world, impacting an estimated 20 million people and affecting 200,000 children worldwide.[1,2] Although advances in cataract surgery have allowed this operation to become a routine procedure for vision restoration, children and patients with uveitis have increased inflammation and fibrin scarring in response

to intraocular surgery, yielding additional considerations for surgical and postoperative management.

An exaggerated postoperative immune response and fibrin scar can lead to formation of a pupillary membrane or displacement of the pupil resulting in occlusion of the visual axis, thereby still potentially limiting the child's vision because of deprivational amblyopia.[3] Balancing amblyopia due to the cataract during the critical period of vision development with potential complications is also considered when the surgeon decides whether to place an intraocular lens (IOL) at the time of surgery, as done with adults, or leave the patient without a lens (aphakic) with the use of contact lenses to correct the refractive error to manage the risk of refractive amblyopia. IOL placement at the time of lensectomy in young children is not usually performed, as there is a greater risk for postoperative complications, so these children are often left aphakic.[4] When aphakia necessitates the use of a contact lens because spectacles are not a practical option, there is a considerable burden on caregivers to insert, remove, and care for the contact lenses. As many as 18% of patients with aphakia experience a contact lens–related adverse event such as corneal abrasion, ulcer, or keratitis.[5] The Infant Aphakia Treatment Study, a randomized clinical trial, compared these two types of treatment (aphakia vs. IOL insertion) and observed that subjects treated with an IOL needed more surgeries in the first postoperative year secondary to complications.[6] Of the 57 subjects with IOL replacement, 17 had pupillary membranes and 11 had corectopia, whereas in the aphakic group only one subject had corectopia.[6] Although visual outcomes were similar, preventative or curative treatments for these complications associated with IOL replacement may reduce visually significant complications and therefore improve visual outcomes for children after cataract.

Uveitis is another condition that may not be amenable to primary IOL implantation with cataract surgery. Cataracts can result as a complication of uveitis, and when surgery is performed these patients need aggressive antiinflammatory management prior to and following surgery to prevent complications.[7–9] Notably, cataracts also occur in up to 52% of children with chronic uveitis.[10] Postoperative complications for patients with uveitis include recurrence of inflammation, fibrin formation (10%), posterior synechiae (46%), posterior capsular opacification (23%–96%), and cystoid macular edema (21%–50%).[11–13]

Our research group seeks to (1) further understand the mechanisms contributing to ocular inflammation and fibrin formation, and (2) investigate prevention and treatment options to ameliorate postoperative adverse events and additional surgeries after intraocular surgery. Our laboratory utilizes a juvenile rabbit animal model to investigate the response following intraocular surgery.[14,15] Juvenile rabbits have a robust immune and fibrotic response following lensectomy with IOL insertion, making them an ideal animal for studying treatment outcomes following intraocular surgery. Sampling of the aqueous humor (AH) before and after a surgical intervention can help deduce the mechanisms and proteins responsible for the exaggerated immune response.

In this work, we investigate the use of tissue plasminogen activator (tPA), which is currently used to dissolve blood clots that cause ischemic stroke, as treatment to reduce intraocular fibrin scarring that has already formed following surgery in our rabbit model. The differences in abundance of inflammatory and fibrotic proteins were also measured in response to intraocular tPA treatment for fibrin scarring. tPA is a serine protease that facilitates the conversion of plasminogen to plasmin, an enzyme that can help reduce the size of a fibrin scar.[16,17] Administration of intraocular tPA has been previously reported for management of fibrin formation in the anterior segment.[18–21] Mehta and Adams[22] documented resolution of the fibrin membrane following the use of 25 µg of tPA following pediatric cataract extraction with IOL insertion. Siatiri and colleagues[23] noted that prophylactic intracameral tPA prevented fibrin membrane for 2 weeks following cataract removal. Furthermore, a low dose (3 µg) of tPA has also been shown to successfully resolve posterior synechiae in patients with acute uveitis.[24] Although these trials and case reports suggest the potential for safe and efficacious use of tPA in the anterior chamber, the changes of the ocular proteome and the abundance changes of inflammatory and coagulation proteins following tPA administration remain uncharacterized.

Using mass spectrometry (MS), we have previously shown that several coagulation factors and inflammatory proteins are significantly increased in abundance in the AH following lensectomy using our rabbit animal model.[14] In this current study, we determine changes in protein abundance of 33 proteins 24 hours following tPA administration. By understanding these abundance changes, we gain insights regarding the effect of tPA on the ocular proteome and which pathways may contribute to postoperative complications. To our knowledge, this study is the first to quantify proteins related to coagulation and fibrin formation in the aqueous humor with and without pharmacological administration in a juvenile rabbit model, thus providing insights into proteomic response to tPA within the anterior chamber.

Determining how the ocular proteome responds to pharmacotherapies builds upon our previous work establishing the ocular proteome in an untreated rabbit model.[14]

Additionally, we establish a novel, objective, quantitative method for measuring fibrin scar volume reduction following treatment with tPA using magnetic resonance imaging (MRI), data necessary for objective and quantitative assessment of therapies designed to prevent or eliminate fibrin scarring in the anterior chamber.

Methods

Animal Preparation and Lensectomy

All experiments were approved by and in compliance with the Institutional Animal Care and Use Committee at the Medical College of Wisconsin. A total of 27 New Zealand White rabbits (Kuiper Rabbit Ranch, Gary, IN), 6 to 7 weeks of age and weighing between 600 and 900 g, were housed in a 14-hour light/10-hour dark cycle and fed a diet of pelleted chow (Laboratory Rabbit Diet High Fiber 5326; LabDiet, St. Louis, MO) daily and a Timothy hay cube twice per week (Bio-Serv, Flemington, NJ). Based on previous studies with preventative pharmacologic therapies where five or six rabbits per group showed significant postoperative differences clinically and in AH proteins,[14,15] eyes of either male or female sex per group were chosen to be randomized to the tPA or control balanced salt solution (BSS) group for postoperative treatments (described below). Rabbits were anesthetized with isoflurane (5% induction, 2.5%–4% maintenance) with 2 L/min of oxygen for surgery and postoperative exams. Eyes were topically anesthetized with 0.5% tetracaine hydrochloride (Bausch + Lomb, Bridgewater, NJ) and dilated with 1% tropicamide and 2.5% phenylephrine (Akorn Pharmaceuticals, Lake Forest, IL) before all procedures. The surgical technique, as described below, was standardized for every procedure, and the same surgeon performed all of the procedures for each experiment. The eye was prepped with 5% betadine solution (Alcon Laboratories, Fort Worth, TX) into the eye. The surrounding area was prepped with 10% betadine and then draped. Preoperative AH samples were collected via corneal paracentesis with a 27-gauge needle on a 1-mL tuberculin syringe. Preoperative AH samples were placed on ice and divided into 25-mL aliquots. Samples were frozen at –80°C until further analysis.

For lensectomy surgery, the anterior chamber was reformed with viscoelastic on a 27-gauge needle (Keralon V++; Keragenix, Rapid City, SD). A clear corneal incision was made just anterior to the limbus using a 20-gauge microvitreoretinal blade. A cystotome needle was used to puncture the anterior capsule followed by micro-utrata forceps to make a continuous curvilinear capsulorhexis. The lens was then removed by irrigation and aspiration with BSS Sterile Irrigating Solution (Alcon Laboratories) via a Simcoe double-lumen irrigation/aspiration cannula. No additional medications were added to the solution. The anterior chamber and capsular bag were then filled with viscoelastic, and the wound was expanded with a 2.4-mm keratome blade. A 10-0 nylon mattress suture was preplaced into the corneal wound. A +30-diopter acrylic foldable intraocular lens (Alcon Laboratories) was inserted into the capsular bag. The viscoelastic was removed with Simcoe irrigation and aspiration. The preplaced suture was tied to close the wound, and the knot was buried. One injection of sustained-release subcutaneous buprenorphine (0.1 mg/kg) was given at the very end of the procedure for analgesia. The rabbit was awakened from anesthesia with topical erythromycin used twice daily for 4 days.

Clinical Examinations and tPA Administration

Postoperatively, rabbits were examined under sedation with isoflurane on postoperative day 3 (POD3). POD3 was chosen because (1) we previously classified this day as the peak of the postoperative response, and (2) it allowed us to compare outcomes with our previous clinical and proteomic studies.[14,15] The intraocular pressure (IOP) in each eye was measured using a TonoLab tonometer (Icare USA, Raleigh, NC). Slit-lamp biomicroscopy (SL-D8Z Digital-Ready Zoom Slit Lamp; Topcon Medical Systems, Oakland, NJ) was performed with photographs obtained using a Nikon D810 camera (Nikon USA, Melville, NY) to evaluate each eye in the categories of iris synechiae, pupil dilation in millimeters, and presence or absence of hemorrhage in the anterior chamber. Anterior chamber inflammation was measured using cell and flare grade as per the Standardization of Uveitis Nomenclature classification system criteria.[25] Following slit-lamp examination on POD3, AH fluid was collected from the anterior chamber by corneal paracentesis. Immediately after AH collection, 100 µL of either 25 µg of recombinant rabbit tPA (Molecular Innovations, Novi, MI) or 100 µL of BSS (control) was injected intracamerally into the anterior chamber. A total of 13 rabbits (six male, seven female) received intracameral tPA, and 14 rabbits (six male, eight female) received intracameral BSS control. Approximately 24 hours following tPA or BSS injection (POD4), rabbits underwent slit-lamp

examination and AH sample collection. Paired clinical data (cell, flare, and IOP measurements for POD3 and POD4 exams) were documented in 15 of 27, rabbits, and paired AH sample collection was obtained in 20 of 27 rabbits. Following AH sample collection on POD4, rabbits were then euthanized with intravenous Fatal-Plus (Vortech Pharmaceuticals, Dearborn, MI) until death was confirmed by absence of respiration, cardiac function, corneal reflex, muscle tone, and mucus membrane color. The entire globe was harvested and placed in 10% neutral-buffered formalin for at least 1 week.

Tesla Magnetic Resonance Imaging

Following formalin fixation, we sought to determine the approximate volume of fibrin reduction in the anterior chamber between tPA-treated eyes and control eyes using magnetic resonance imaging (MRI). To stabilize the eye for imaging, the fixed eye was placed in the center of a 50-mL conical tube containing a 1% agarose gel. The eye was scanned using a BioSpec 94/20 USR preclinical MRI system (Bruker Biospin, Billerica, MA) with a 32-mm Litz birdcage coil (Doty Scientific, Columbia, SC). Images were acquired using T1-weighted gradient-echo imaging with inversion recovery with the following settings: slice thickness, 182.5 µm (except rabbit 31823, which had a slice thickness of 160 µm); echo time, 14.03 ms; repetition time, 1300 ms; inversion time, 500 ms; number of signal averages, nine (rabbits 31823, 31931, 31932, and 31934 had 10 signal averages); imaging frequency, 400 MHz; number of phase-encoding steps, 120; echo train length, 8; and pixel bandwidth, 558 (except for rabbit 32001, which had a pixel bandwidth of 279.017). Images were viewed using Horos Project software.[26] Using the pencil tool, the area of the fibrin scar observed in each slice was measured by three masked observers and then multiplied by slice thickness to determine the total fibrin volume (see Supplementary Fig. S1). Observers were allowed to view the corresponding slit-lamp image when drawing fibrin measurements. Supplementary Table S1 contains all of the MRI settings for each scan.

Targeted Quantitation of Proteins of Interest Using Tandem MS

The AH from a total of 12 rabbits was analyzed by MS, with six POD4 samples coming from tPA-treated rabbit eyes and six samples from control rabbit eyes. Then, 10 µL of each AH sample was aliquoted and diluted with 100-mM ammonium bicarbonate, 40% Invitrosol (Thermo Fisher Scientific, Waltham, MA), 20% acetonitrile (MeCN), and 5.52-mM *tris*(2-carboxyethyl)phosphine (TCEP) to bring the samples to the final concentration of TCEP to 5 mM for reduction. Samples were then incubated for 30 minutes at 1400 rpm at 25°C in a thermomixer (Eppendorf, Hamburg, Germany). Then, 100-mM iodoacetamide was added to bring samples to 10 mM for alkylation; they were then mixed in the dark for 30 minutes at 1400 rpm at 37°C in a thermomixer. Pierce Trypsin/Lys-C Mix (Thermo Fisher Scientific) was added at a trypsin-to-protein ratio of 1:20 for overnight incubation (~18 hours) at 37°C and 1400 rpm in the thermomixer. Sera-Mag SpeedBead Carboxylate-Modified Magnetic Particles (hydrophilic and hydrophobic; GE Healthcare Life Sciences, Sheffield, UK) were prepared at a 1:1 ratio to create a particle suspension, and peptides were prepared for proteomic analysis using the SP2 method as previously described.[27] Briefly, 8 µL of particle solution was added to the samples to create a 20:1 particle-to-peptide ratio, and 100% MeCN was added to bring the final concentration of MeCN to 95%. Samples were mixed by pipetting up and down three to five times to make sure the particles were well dispersed, allowed to settle for 2 minutes, and placed on a magnetic rack. The supernatant was removed, and particle-bound samples were washed with 100% MeCN to cover the particles completely. Samples were returned to the magnetic rack and allowed to sit for 60 seconds. Next, another 100% MeCN wash was performed and the supernatant discarded. The particles were then reconstituted in a solution consisting of 2% MeCN and water, vortexed, and allowed to settle for 1 minute. The supernatant (now containing the peptides) was collected and transferred to a new microfuge tube. Samples were then acidified with 10% formic acid for a final concentration of 0.1% acid. The sample was then spun at 14,000 rpm for 10 minutes and the supernatant was collected.

The peptides were quantified using a Pierce Quantitative Fluorometric Peptide assay (Thermo Fisher Scientific), and each sample was diluted to 25 ng/µL in 2% MeCN with 0.1% formic acid. Peptide Retention Time Calibration Mixture (Thermo Fisher Scientific) was added to each sample at a final concentration of 4 nM to enable retention time calibration and assessment of instrument performance throughout acquisition. Equal volumes of each sample were combined into a single, pooled quality-control mixture.

Based on a previous study,[14] proteins related to coagulation, complement cascades, and unrelated proteins (as control proteins) were analyzed by MS. A summary of these methods is provided in Supplementary Fig. S4. Targeted quantitation by parallel reaction monitoring was performed using a Dionex UltiMate 3000 RSLCnano system inline with an

Orbitrap Fusion Lumos Tribrid MS (Thermo Fisher Scientific). Samples (as single replicate injections) were queued in a randomized order. Each peptide was scheduled with a set 10-minute scheduled retention time window, and resulting MS data were processed using Skyline 20.2.1.[28] Retention times and ions were manually aligned and selected. Selected peptides and ions are reported in Supplementary Table S2 and on Skyline Panorama (panoramaweb.org/YN6kGa.url). All liquid chromatography, instrumentation, and data processing settings can be found in Supplementary Tables S3 and S4, and all RAW files and other relevant data files are publicly available at Skyline Panorama. Identification of uncharacterized proteins or those with generic domains (such as cystatin domain-containing protein) was further validated by performing a protein Basic Local Alignment Search Tool (BLAST) analysis of the FASTA sequence.[29]

Statistics

All statistical comparisons were performed using Prism 9.0.0 (GraphPad, San Diego, CA). Categorical data assessments of cell and flare were compared using the Wilcoxon matched-pairs signed-rank test. Observer comparisons between the MRI measurements were compared using a repeated-measures, one-way analysis of variance (ANOVA) test, with Greenhouse–Geisser correction. Following this comparison, an unpaired *t*-test with Welch correction was performed to compare the volume of the fibrin scar between tPA and control-treated eyes. All MS data were exported from Skyline and processed in MSstats[30] using the settings found in Supplementary Table S4. MS data were analyzed using with one-way ANOVA followed by Tukey's test.

Results

Slit-Lamp and MR Imaging

Following IOL insertion in the juvenile rabbit, untreated eyes had a large amount of fibrin observed within the anterior chamber (Figs. 1A, 1D). Twenty-four hours after an injection of BSS (control), a large fibrin scar remained visible on slit-lamp imaging (Fig. 1B) and was observed anterior to the IOL when assessed via ex vivo MRI (Fig. 1C). However, after tPA was injected on POD3, the fibrin scar dissolved (Fig. 1E), and a significant reduction of the volume of fibrin was consequently seen via MRI (Fig. 1F).

Clinical exams revealed significant increases in the cell observed in the anterior chamber of tPA-treated eyes ($P < 0.05$) (Fig. 2A) but not in control eyes ($P > 0.99$) (Fig. 2B). No significant differences were observed in anterior chamber flare between

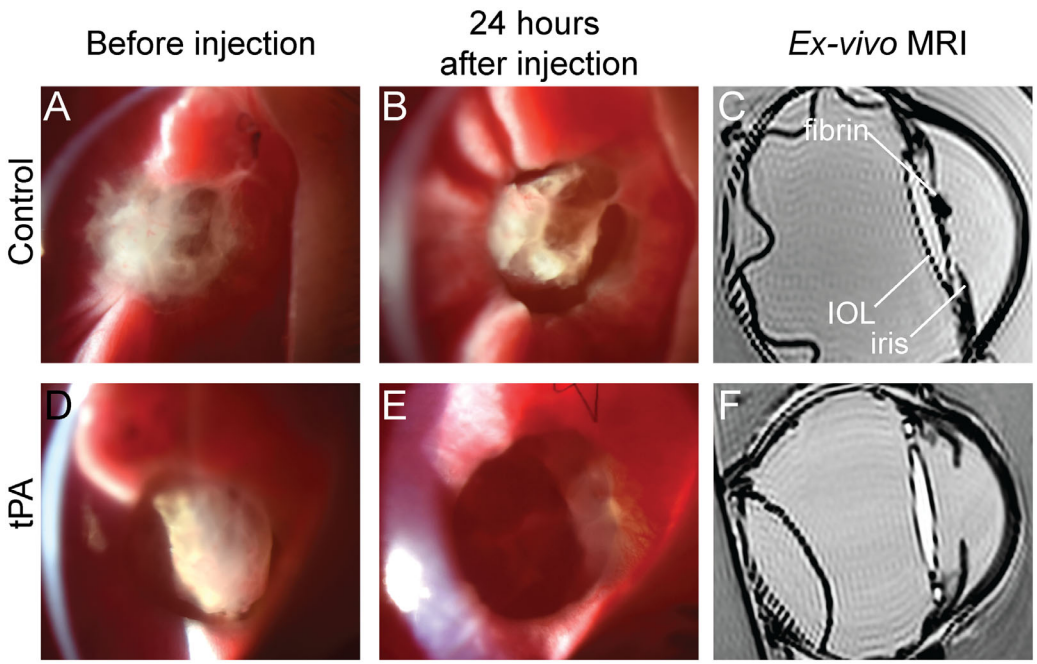

Figure 1. Clinical examinations following lensectomy with IOL insertion with and without tPA treatment in a juvenile rabbit model. Representative color pictures of rabbit eyes following lensectomy with IOL insertion before injection on POD3 (**A, D**) and 24 hours after injection (POD4) of BSS (control, **B**) or tPA (**E**). MR images corresponded with clinical photographs, and a large mass of fibrin scar was observed in front of the IOL (**C**) but was not detected on the tPA-treated eye (**F**).

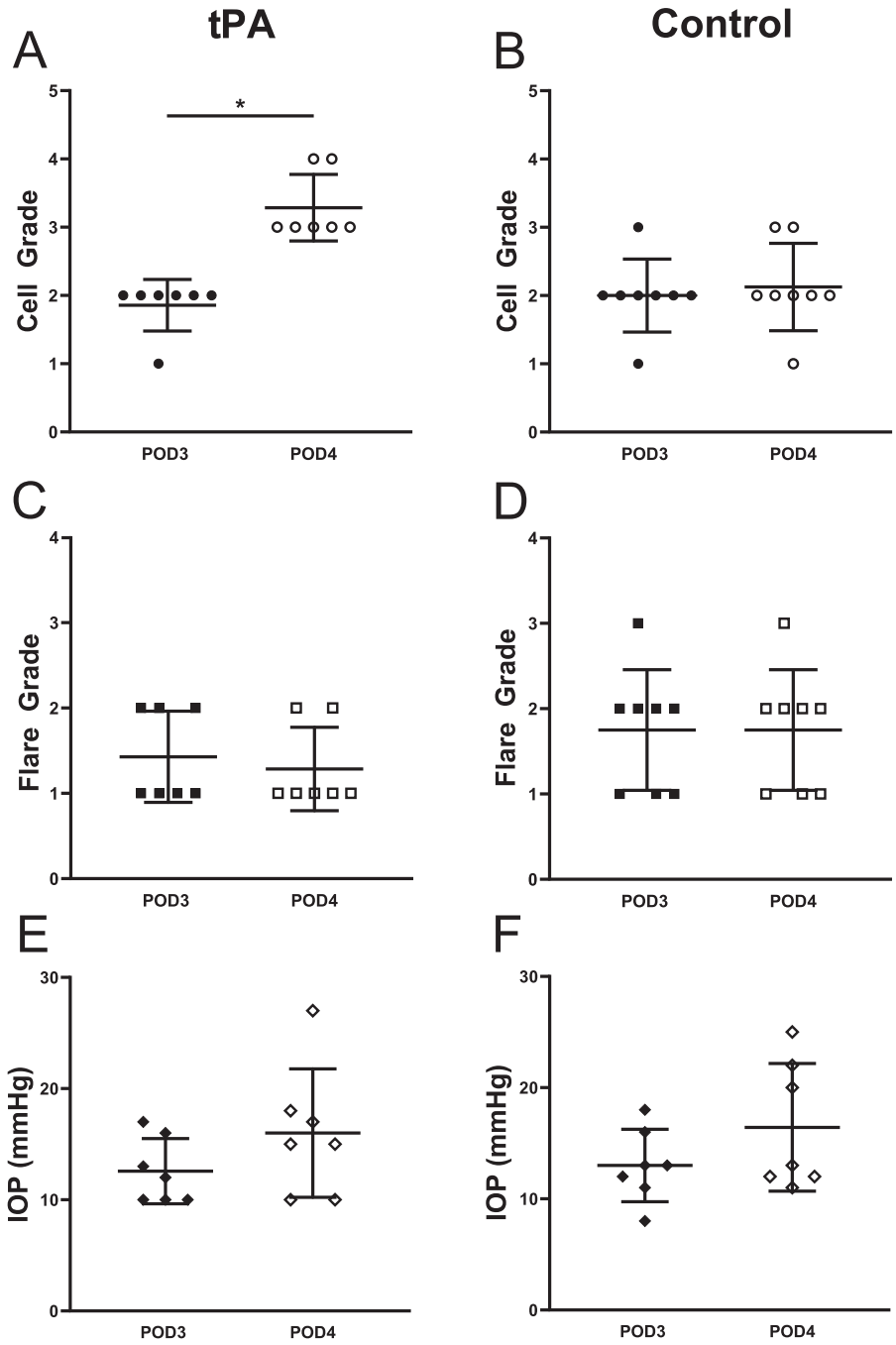

Figure 2. Cell, flare, and IOP clinical measurements. (**A**) Following tPA administration into the anterior chamber, there was a significant increase in cell grade detected after 24 hours ($P < 0.05$; POD4). (**B**) This increase, however, was not observed in control eyes. Administration of tPA did not result in any significant changes in flare grade when compared with controls (**C, D**). Paired assessments of IOP revealed no significant changes in IOP following injections of tPA (**E**) or BSS.

tPA-treated eyes ($P > 0.99$) (Fig. 2C) and control eyes ($P > 0.99$) (Fig. 2D). Additionally, significant changes were not observed in IOP following tPA treatment or control injection (Figs. 2E, 2F).

For MRI analyses, there was no significant difference between the measurements of fibrin volume among the three masked observers for control or tPA-treated eyes (Fig. 3A). Because there was no significant difference among the observers for the volumetric measurements, the final volume measurement for each eye was an average of the measurements from the three observers. The fibrin volume was then compared

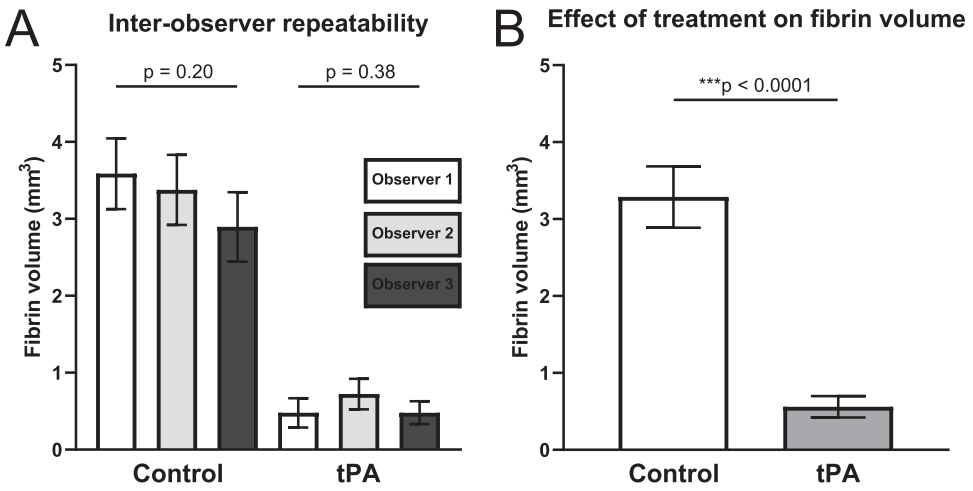

Figure 3. MRI fibrin volume. (**A**) There was no significant difference among the observations of the masked observers when assessing control eyes (average ± SEM; $F = 1.72$; $P = 0.2021$) or tPA-treated eyes ($F = 1.01$; $P = 0.3765$). (**B**) The average value of fibrin volume was then calculated using an average of the three measurements for each eye. There was a significant decrease in fibrin scar volume in tPA-treated eyes versus control eyes (average ± SEM; Welch-corrected $t = 6.46$; $P < 0.0001$).

between control eyes and tPA eyes, with a significant decrease found in eyes treated with tPA (Fig. 3B). Eyes were fixed for a variable number of days prior to imaging, ranging from 7 to 299 days; however, the time of fixation was not correlated with the size of the fibrin scar (Supplementary Fig. S2).

Targeted MS

Three days after lensectomy with IOL placement (POD3), a variety of proteins related to the coagulation and the complement cascade increased in abundance compared with preoperative samples but prior to any drug intervention (complement C1q C chain, coagulation factors V and X) (Fig. 4A). Several proteins related to fibrin scarring and inflammatory processes also decreased in abundance following surgery (such as alpha-2-macroglobulin, alpha-2-plasmin inhibitor, and complement component 7). The specific abundances of the fibrinogen alpha chain, beta chain, and gamma chain, proteins which comprise the fibrin scar,[31] are provided. Although significant increases in abundance were observed starting on POD3, these proteins remained elevated with and without tPA administration (Fig. 4B), despite resolution of the fibrin scar on clinical imaging (Fig. 1E).

Additional proteins assessed by targeted MS require further investigation to decipher their exact role in the postoperative response to lensectomy with IOL (Supplementary Fig. S3). Afamin, carboxylic-ester hydrolase, extracellular matrix protein 1, lumican, and serum paraoxanase were proteins detected in previous analyses that did not significantly change in abundance following lensectomy with IOL insertion at POD3.[14] Although serum paraoxanase decreased slightly compared to preoperative levels, these proteins remained relatively consistent in their abundance before and after surgery, thus rendering them potential control proteins to assess the quality of a MS sample.

Discussion

Postoperative management of pediatric cataracts presents difficult options for ophthalmologists as they consider the lifelong implications of vision for the child. Restoring a clear visual axis as soon as possible can improve visual outcomes and decrease deprivational amblyopia. In addition, patients with uveitis that are in need of cataract surgery also have increased likelihood of postoperative complications, including fibrin scarring and increased inflammation.[7] In order to reduce the fibrin scar, we investigated the use of tPA in a juvenile rabbit model, where the inflammatory response and fibrin formation are typically more severe than those observed in a child. Previous literature has reported the use of tPA in three patients with uveitis and posterior synechiae on maximum antiinflammatory therapy.[24] This work provides additional data that tPA is an effective treatment for ocular fibrin scarring, leading to improved clinical outcomes, while also establishing quantitative proteomic data for fibrotic and inflammatory proteins that may contribute to postoperative complications.

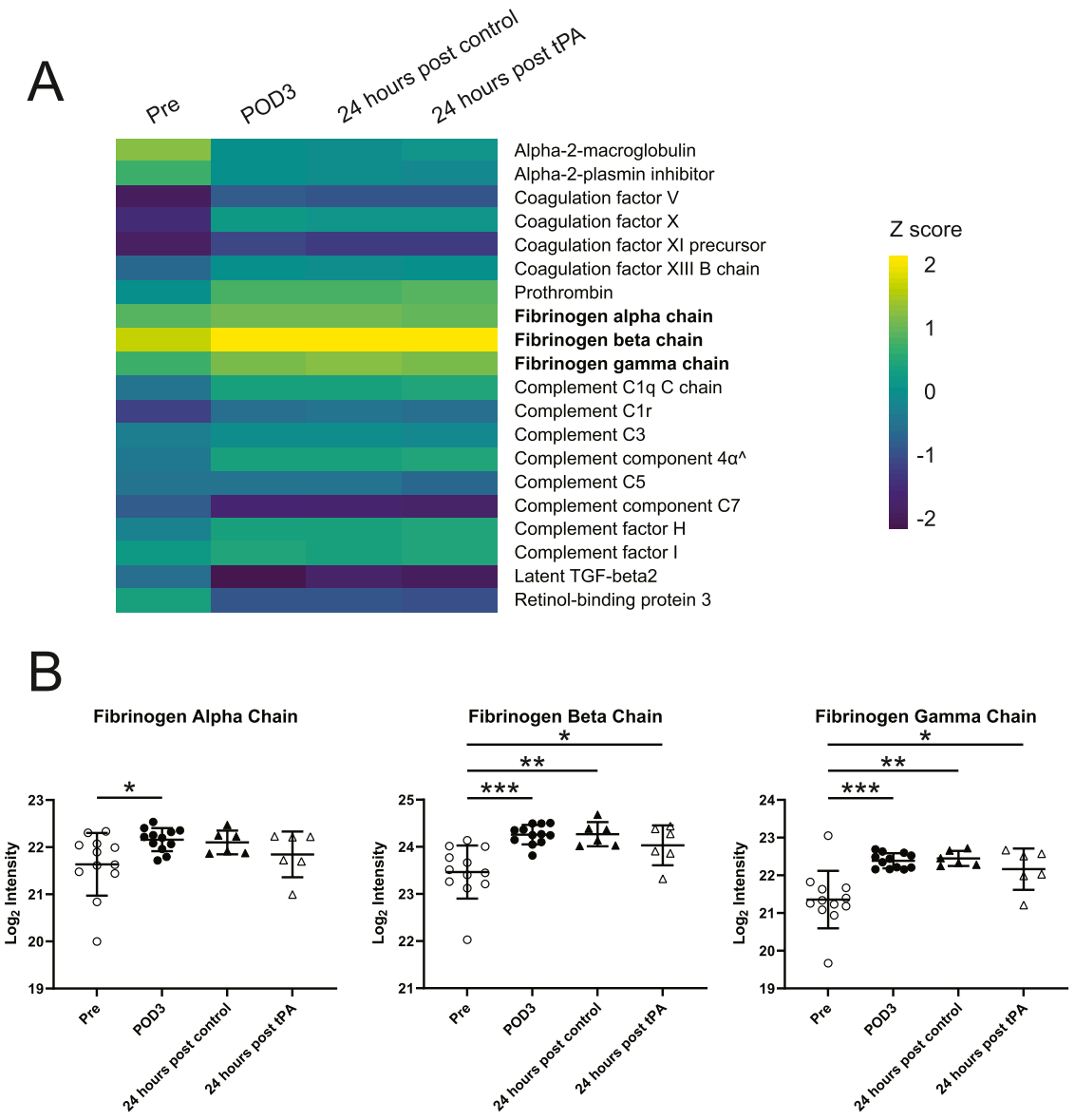

Figure 4. Protein abundances assessed by targeted MS. (**A**) Heat map of proteins relative to preoperative samples at POD3 (prior to intervention), as well as 24 hours after control injection and 24 hours after tPA administration (POD4). Proteins related to the coagulation pathway and complement cascade generally increased in abundance. Following BSS (control) injection and tPA administration, proteins remained elevated despite improvements in clinical images. The *z*-score for each protein for each condition was calculated by taking the protein abundance in one condition minus the mean of that one protein among all conditions and dividing that value by the standard deviation of that one protein among all conditions. The specific abundance values of the fibrinogen proteins are *bolded* and provided in (**B**). Significant differences were observed comparing preoperative levels (Pre) to levels 3 days after surgery (POD3) (average ± SD; $^{*}P < 0.05$, $^{**}P < 0.01$, $^{***}P < 0.001$), but no differences were observed 24 hours after tPA treatment compared with the control groups (POD4). A *carrot* (^) denotes complement component 4 binding protein alpha.

In order to quantify the volume of fibrin reduction with administration of 25 µg of tPA, we used 9.4-Tesla MRI to measure the amount of fibrin in the anterior chamber. This imaging technique provides an additional resource to fully approximate the fibrin volume to supplement the slit-lamp imaging. By fixing the entire eye, the globe remains intact, keeping the fibrin secure inside of the anterior segment. Although fibrin can be detected in rabbit eyes using paraffin embedding,[15] the process of dehydration and sectioning makes this method challenging for quantifying the total volume of fibrin inside of the eye, which led us to pursue MRI. Although the masked observers measurements varied slightly in identifying the approximate regions of fibrin (Fig. 3A), there were no significant differences among the measurements. The efficacy of

administering 25 µg of tPA into the anterior chamber can be observed in Figure 3B. MRI provides an excellent platform for quantitative measurement of the postoperative fibrin scar and may be useful in future dose–response studies to define the minimum amount of drug for maximum fibrin-reducing effect.

The fibrin scar is formed by the cleavage of fibrinogen, which is composed of the fibrinogen alpha, beta, and gamma chains.[31] In previous work, we performed histological analysis confirming the content of the scar as containing fibrin throughout.[15] The formation of fibrin can occur via the intrinsic and extrinsic coagulation pathways,[32] ultimately resulting in conversion of the protein prothrombin to thrombin, which can then cleave fibrinogen to fibrin. We hypothesized that a decrease in the fibrin scar would consequently result in a decrease of the fibrin-related proteins. However, we suspect that, upon administration of tPA, the fibrin components (and fibrin degradation products) remained in a soluble form in the anterior chamber and were collected on the POD4 sample. Furthermore, the observed increases in the amount of cell within the anterior chamber (Fig. 2A) may be explained as fibrin degradation products upon dissolution of the fibrin scar. Although these degradation products remain in the anterior segment and are likely collected in the sample, we do not believe these proteins would reform into the complex fibrin matrix due to the intricate cascade necessary for fibrin formation.

In addition to the coagulation factors and fibrinogen chains, a variety of complement components increased in abundance compared with preoperative levels (Fig. 4A). Despite the significant clinical improvement, complement proteins also remained elevated following the treatment injection. Based on the interactions between the coagulation and complement systems,[33] we hypothesized that complement proteins would decrease in abundance along with the anticipated decrease in fibrinogen chains, but this was not observed. Future studies should investigate a longer postoperative time point to determine if fibrotic, complement, and coagulation proteins remain persistently elevated following treatment. Collection of AH fluid at longer time points would potentially allow a longer period for soluble fibrin to be cleared out of the anterior chamber via turnover and production of aqueous humor, thus potentially leading to lower amounts of the protein being detected following treatment, which may also correlate with changes in inflammatory proteins.

The eye is a unique environment because it is an immune-privileged site. In this case, the ocular immune system must guide its response between the elimination and neutralization of the pathogen while also avoiding immunopathogenic tissue injury that interferes with vital functions.[34] In order to prevent excessive inflammation in the anterior segment of the eye, the AH contains factors that maintain an ocular immunosuppressive environment, such as transforming growth factor-beta 2 (TGF-β2). We previously reported the hypothesis that loss of ocular immunosuppressive proteins, such as TGF-β2, latent TGF-β2, and potentially retinol-binding protein 3, may contribute to excessive postoperative scarring and inflammation. In this work, we noticed a decrease in latent TGF-β2 and retinol-binding protein 3 following surgery compared with preoperative levels, and these proteins remained decreased in abundance following treatment or control administration (Fig. 4A). Improved clinical outcomes did not imply a restored abundance of these specific factors.

Although informative regarding the mechanisms of tPA within the anterior chamber, this study did have a number of limitations. The time of eye fixation prior to MRI was not consistent, but there was no relationship between days of fixation and fibrin volume size (Supplementary Fig. S2). A more accurate comparison of fibrin volume reduction would be to use in vivo MRI techniques before and after tPA injection to compare the fibrin scar size within the same rabbit. This would require use of a 7-Tesla magnet (live rabbits would not fit inside the 9.4-Tesla MR scanner) and thus reduce definition of the images. Although this study did use targeted methods of MS to provide high confidence in the quantitative data presented, these data reflect the relative abundance of proteins before and after surgery. Due to limited available amounts of AH sample collected, western blots and enzyme-linked immunoassays were not investigated in this analysis, as that would have required samples from multiple eyes, potentially confounding the data. Additional targeted studies using labeled peptides would provide further reliable quantification regarding changes in protein levels. Last, this study considered only the proteins in the AH measured at postoperative days three and four (24 hours after treatment or control injections), and later postoperative time points are recommended, as previously mentioned. Despite these limitations, this work provides further evidence that tPA may be a safe and effective treatment option for eliminating the fibrin membrane as we work toward developing pharmacotherapies to reduce postoperative complications associated with uveitic and pediatric intraocular surgery. Investigating how the ocular proteome changes at different surgery steps,[14] with pharmacological treatment (this work), and with age (future directions) will provide critical insights that will help reveal

the underlying cause of the exaggerated ocular immune response in children and identify which pharmacotherapies offer the best visual outcomes.

Acknowledgments

The authors thank Michael Pereckas (Center for Biomedical Mass Spectrometry Research, Medical College of Wisconsin) for all of his assistance regarding sample preparation and analysis for the mass spectrometry components of this work.

Supported by grants from the National Eye Institute, National Institutes of Health (K08EY024645 to ISK, P30EY001931, and C06RR016511). Additional support was also provided by Children's Research Institute and the Daniel M. Soref Charitable Trust, as well as the National Institutes of Health (TL1TR001437 and UL1TR001436 to LBL), American Heart Association (20PRE35200049 to LBL). LBL is a member of the Medical College of Wisconsin Medical Science Training Program, which is partially supported by a T32 grant from the National Institute of General Medical Sciences (GM080202). Funding sources were not involved in the study design, data collection, interpretation, analysis, or publication of results. The sponsors or funding organizations had no role in the design or conduct of this research.

Disclosure: **J.B. Young**, None; **A.R. Buchberger**, None; **J.D. Bogaard**, None; **L.B. Luecke**, None; **M. Runquist**, None; **C.M.B. Skumatz**, None; **I.S. Kassem**, None

References

1. Pascolini D, Mariotti SP. Global estimates of visual impairment: 2010. *Br J Ophthalmol*. 2012;96:614–618.
2. Foster A, Gilbert C, Rahi J. Epidemiology of cataract in childhood: a global perspective. *J Cataract Refract Surg*. 1997;23(suppl 1):601–604.
3. Gremida A, Kassem I, Traish A. Anterior capsular rupture following blunt ocular injury. *Digit J Ophthalmol*. 2011;17:66–68.
4. Trivedi RH, Wilson ME. Pediatric cataract surgery with an intraocular lens implant. *Expert Rev Ophthalmol*. 2007;2:819–832.
5. Lambert SR, Lynn MJ, Hartmann EE, et al. Comparison of contact lens and intraocular lens correction of monocular aphakia during infancy: a randomized clinical trial of HOTV optotype acuity at age 4.5 years and clinical findings at age 5 years. *JAMA Ophthalmol*. 2014;132:676–682.
6. Plager DA, Lynn MJ, Buckley EG, Wilson ME, Lambert SR, Infant Aphakia Treatment Study Group. Complications, adverse events, and additional intraocular surgery 1 year after cataract surgery in the infant Aphakia Treatment Study. *Ophthalmology*. 2011;118:2330–2334.
7. Guindolet D, Dureau P, Terrada C, et al. Cataract surgery with primary lens implantation in children with chronic uveitis. *Ocul Immunol Inflamm*. 2018;26:298–304.
8. Quinones K, Cervantes-Castaneda RA, Hynes AY, Daoud YJ, Foster CS. Outcomes of cataract surgery in children with chronic uveitis. *J Cataract Refract Surg*. 2009;35:725–731.
9. Yangzes S, Seth NG, Singh R, et al. Long-term outcomes of cataract surgery in children with uveitis. *Indian J Ophthalmol*. 2019;67:490–495.
10. Rosenberg KD, Feuer WJ, Davis JL. Ocular complications of pediatric uveitis. *Ophthalmology*. 2004;111:2299–2306.
11. Baheti U, Siddique SS, Foster CS. Cataract surgery in patients with history of uveitis. *Saudi J Ophthalmol*. 2012;26:55–60.
12. Suresh PS, Jones NP. Phacoemulsification with intraocular lens implantation in patients with uveitis. *Eye (Lond)*. 2001;15:621–628.
13. Chiu H, Dang H, Cheung C, et al. Ten-year retrospective review of outcomes following phacoemulsification with intraocular lens implantation in patients with pre-existing uveitis. *Can J Ophthalmol*. 2017;52:175–180.
14. Young JB, Keppel TR, Waas M, et al. Quantitative proteomic analysis of aqueous humor after rabbit lensectomy reveals differences in coagulation and immunomodulatory proteins. *Mol Omics*. 2020;16:126–137.
15. Bogaard JD, Young JB, Movahedan A, Kassem IS. Use of a juvenile rabbit animal model to evaluate therapeutic interventions for postoperative inflammation and fibrin formation after lensectomy. *Transl Vis Sci Technol*. 2019;8:5.
16. Jilani T, Siddiqui AH. *Tissue Plasminogen Activator*. Treasure Island, FL: StatPearls; 2021.
17. Tripathi RC, Tripathi BJ. Tissue plasminogen activator therapy for the eye. *Br J Ophthalmol*. 2005;89:1390–1391.
18. Tripathi RC, Tripathi BJ, Bornstein S, Gabianelli E, Ernest JT. Use of tissue plasminogen activator for rapid dissolution of fibrin and blood clots in the eye after surgery for glaucoma and

cataract in humans. *Drug Dev Res*. 1992;27:147–159.
19. Tripathi RC, Tripathi BJ, Park JK, et al. Intracameral tissue plasminogen activator for resolution of fibrin clots after glaucoma filtering procedures. *Am J Ophthalmol*. 1991;111:247–248.
20. Snyder RW, Sherman MD, Allinson RW. Intracameral tissue plasminogen activator for treatment of excessive fibrin response after penetrating keratoplasty. *Am J Ophthalmol*. 1990;109:483–484.
21. Jaffe GJ, Abrams GW, Williams GA, Han DP. Tissue plasminogen activator for postvitrectomy fibrin formation. *Ophthalmology*. 1990;97:184–189.
22. Mehta JS, Adams GG. Recombinant tissue plasminogen activator following paediatric cataract surgery. *Br J Ophthalmol*. 2000;84:983–986.
23. Siatiri H, Beheshtnezhad AH, Asghari H, Siatiri N, Moghimi S, Piri N. Intracameral tissue plasminogen activator to prevent severe fibrinous effusion after congenital cataract surgery. *Br J Ophthalmol*. 2005;89:1458–1461.
24. Lerner LE, Patil AJ, Kenney MC, Minckler D. Use of intraocular human recombinant tissue plasminogen activator as an adjunct treatment of posterior synechiae in patients with uveitis. *Retin Cases Brief Rep*. 2012;6:290–293.
25. Jabs DA, Nussenblatt RB, Rosenbaum JT, Standardization of Uveitis Nomenclature (SUN) Working Group. Standardization of uveitis nomenclature for reporting clinical data. Results of the First International Workshop. *Am J Ophthalmol*. 2005;140:509–516.
26. Horos Project. Horos Project. Available at: Horosproject.org. Accessed September 16, 2021.
27. Waas M, Pereckas M, Jones Lipinski RA, Ashwood C, Gundry RL. SP2: rapid and automatable contaminant removal from peptide samples for proteomic analyses. *J Proteome Res*. 2019;18:1644–1656.
28. MacLean B, Tomazela DM, Shulman N, et al. Skyline: an open source document editor for creating and analyzing targeted proteomics experiments. *Bioinformatics*. 2010;26:966–968.
29. National Center for Biotechnology Information, U.S. National Library of Medicine. BLAST: Basic Local Alignment Search Tool. Available at: https://blast.ncbi.nlm.nih.gov/Blast.cgi. Accessed September 16, 2021.
30. Choi M, Chang CY, Clough T, et al. MSstats: an R package for statistical analysis of quantitative mass spectrometry-based proteomic experiments. *Bioinformatics*. 2014;30:2524–2526.
31. Mosesson MW. Fibrinogen and fibrin structure and functions. *J Thromb Haemost*. 2005;3:1894–1904.
32. Palta S, Saroa R, Palta A. Overview of the coagulation system. *Indian J Anaesth*. 2014;58:515–523.
33. Amara U, Flierl MA, Rittirsch D, et al. Molecular intercommunication between the complement and coagulation systems. *J Immunol*. 2010;185:5628–5636.
34. Streilein JW. Ocular immune privilege: therapeutic opportunities from an experiment of nature. *Nat Rev Immunol*. 2003;3:879–889.